

# **MEASUREMENT OF GAS PERMEABILITIES UNDER DIFFERENT COMPACTION MODES ON TIGHT RESERVOIR SAMPLES**

Ludovic D. JAUMOUILLE (Automatisme et Informatique Appliqués)  
Philippe R. CORDELIER (Elf Aquitaine Production - Reservoir Dpt.)  
Adel KHARROUBI (Ecole des Mines de Paris - ARMINES / CGES)

## **Abstract**

Reliable core measurements of permeability are very important for reservoir engineers predicting, well productivity, and its change versus time. In most laboratories, permeabilities are usually measured under hydrostatic loads that do not reproduce reservoir in-situ conditions (deviatoric stresses, oedometric deformations among others) while failing to simulate the reservoir stress path during production.

For the purposes of comparison, both hydrostatic and uniaxial compactions were applied to low permeability samples [from less than 1 mD to  $10^{-2}$  mD] cored in a carbonate reservoir and in an overpressured sandstone reservoir. As steady state methods are delicate and time consuming for tight rocks, an original and user-friendly unsteady-state gas permeameter was developed. These tests aimed at determining the gradual evolution of permeability and porosity when effective stresses increase over the major depletions contemplated. Results show that permeabilities strongly vary with stress paths. Permeability reductions under uniaxial compactions are 25% to 60% lower when compared to isotropic conditions. Furthermore, the lower the intrinsic permeability, the higher the permeability reduction. Permeability decreases are noticed to be consistent with deformations. This study demonstrates that choosing hydrostatic or uniaxial compactions (the latter being more closely related to actual reservoir conditions) is of the highest importance with respect to low permeability formations evaluation. The difference may become critical for rocks with permeabilities close to the cutoff level.

## **Introduction**

Permeability and porosity are stress-sensitive properties and change with declining reservoir pore pressure, during production, generating effective stresses increase. These factors are usually measured under hydrostatic loads, at ambient pore pressure, that fail to properly simulate both the deviatoric stress state and deformations that prevail in most reservoirs, as well as their evolutions. Moreover, the lower the permeability, the higher the reduction.

Deep, undercompacted, high fluid pressure reservoirs are now the target of our industry (North Sea, Gulf of Mexico). Very large pressure decline will occur when producing their hydrocarbon reserves, which may impair the rock characteristics, and the well productivity. As a consequence, it is of paramount importance to anticipate the change in rock properties induced by the pore pressure drawdown, in order to reliably forecast well productivity versus time.

Two series of experiments were thus designed to determine, on low permeability sandstones and carbonates, the evolution of both matrix permeability and porosity under different loading conditions together with deformation modes, namely uniaxial compaction (i.e. oedometric) tests versus hydrostatic tests, when effective stresses increase. Uniaxial compaction is actually considered to be representative of 80% of petroleum reservoirs discovered. Experiments performed accordingly are therefore useful to calibrate more conventional measurements.

## **Lithology and Sample Selection**

A first series of measurements was carried out on sandstones from an overpressured reservoir. A second series was conducted on carbonate reservoir samples. S-type specimens are feldspathic sandstones, the remaining part (10% to 12%) containing micas and clay minerals (7% to 8%). C-type samples are nearly pure dolomite (96% to 98%). All of them are representative of the reservoirs from which they were cored.

## **Experimental Set-up**

### **Permeability Measurements Facility**

The steady-state method is mainly suited to high permeability cores. For low permeability cores, it is very time consuming and accurate measurements of smaller flow rates through the core are really tricky.

When long testing times are required, environmental changes can introduce errors into the raw data measured. In an effort to solve these laboratory problems, an unsteady-state apparatus was developed for measuring permeability on tight rocks more efficiently.

A schematic diagram of the unsteady-state gas permeameter is given in figure 1. Depending on pore volume of the specimens, either three or two gas chambers are connected respectively at the inlet and the outlet of the core sample. This configuration allows various combinations of volumes. The differential pressure of the fluid (Nitrogen) is measured between the outlet and the inlet of the core sample.

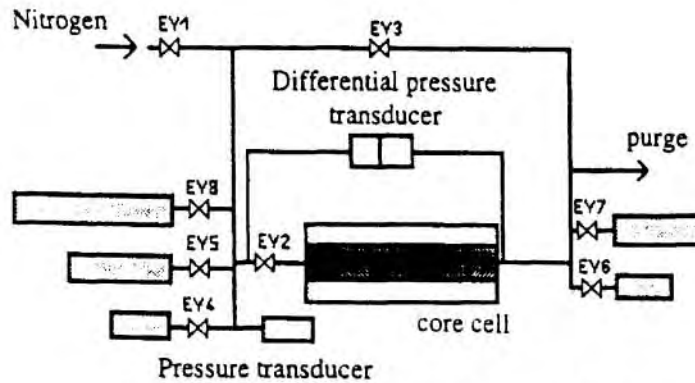


Figure 1 : Unsteady-state gas permeameter

There are two basic configurations : in one case the outlet from the core sample is connected directly to the atmosphere. In the other case the core sample outlet is connected to an other reservoir. As this testing facility is fully computerized from the start, its operation is straightforward. A sample is set in the core holder, the pulse valve "EV2" is closed and source chamber is filled with Nitrogen to 10 bars. At time zero, the pulse valve is opened. The differential pressure is then recorded as a function of time. The experimental method and data analysis procedures are essentially based on Jones's (1991) and Bourbie (1982).

The method provides convenient, rapid and accurate means of determining both gas permeability, corrected from Klinkenberg's effect, and Forcheimer's coefficient.

At low Reynolds numbers the flow is assumed to be laminar, viscous forces are predominant, and Darcy's law is valid. However for gas flooding, Klinkenberg argued that interactions between gas molecules and the walls of porous medium preferentially help the molecules traveling in the direction of the flow, thus increasing gas permeability. The slippage effect is enhanced at lower pore pressures (Mc Phee, C.A., Arthur, K.G., 1991; Ifly, R., 1956). This correction is compulsory for our laboratory measurements for which pore pressure never exceeds 10 bars. Moreover the slippage is as much intense as the permeability is low, hence it takes on a particular importance for the tight rocks selected in this study.

One of the most outstanding features of this testing installation lies in its capability to determine both low permeabilities [from  $10^{-3}$  mD to 10 mD] and high permeabilities [from 10 mD to 400 mD].

Low permeabilities are determined by means of the "Pulse Decay" method which uses upstream and downstream reservoirs. This method reduces inertial effect and is therefore more convenient for low permeabilities.

Higher permeabilities are determined by means of the "Draw-down" method (or pressure falloff), so as to derive the characteristic value of inertial effect : Forcheimer's turbulence factor  $\beta$ .

These methods are based on the following data analyses :

Draw-down : Jones first introduced a pressure drawdown permeameter. The flow through the sample with time is described by the relationship :

$$\frac{V_1}{P_1} \times \frac{dP_1}{dt} = Q(t) \quad (1)$$

Introducing  $P_1$  and  $Q$  into the generalized Darcy's equation :

$$\vec{\text{grad}} P = -\frac{\mu_p}{K_{gkl}} \vec{v} + \beta \rho |\vec{v}| \vec{v} \quad (2)$$

leads to the determination of the gas permeability  $K_g$  and  $\beta$  coefficient.

Pulse Decay : The solution of the diffusion equation is based on the Hsieh P.A. et al.'s original work (1981).

$$\frac{d^2P}{dx^2} - \frac{\mu_p \cdot c_{tp}}{K_g} \times \frac{dP}{dt} = 0 \quad (3)$$

Considering the primary and boundary conditions below, this equation can be solved :

$$P(0,t) = P_2(t) \quad [\text{inlet and outlet of sample are linked to the upstream}$$

$$P(L,t) = P_1(t) ; t > 0 \quad \text{and downstream pressures of the selected reservoirs}]$$

$$\frac{\mu_p \cdot c_{gp}}{K_g A} V_2 \times \frac{dP_2}{dt} - \left(\frac{dP}{dx}\right)_{x=0} = 0 \quad [\text{mass flow conservation}]$$

$$P_2(0) = 0$$

$$\frac{\mu_p \cdot c_{gp}}{K_g A} V_1 \times \frac{dP_1}{dt} - \left(\frac{dP}{dx}\right)_{x=L} = 0$$

... so we get the value of gas permeability. To account for the effect of slippage at the walls ( $K_g = K_{gkl}(1 + b/P_m)$ ), an iterative method (on  $b$ ) is used, based on a model applicable to low permeabilities, developed by Jones.

### Stress Paths - Experimental Procedure

For comparative purposes, both hydrostatic and uniaxial compactions were applied to the samples. Each sample is first loaded under hydrostatic loading conditions up to 1200 bars isotropic stress - S-type samples - (resp. 700 bars - C-type samples -), then unloaded, checked for irreversible deformations with respect to porosity and permeability. Then, sample is loaded again under uniaxial loading conditions ( $\sigma'_a = 0$ ,  $\epsilon'_r = 0$ ), up to 1200 bars axial effective stress - S-type samples - (resp. 700 bars - C-type samples -). Radial strains are carefully monitored to follow the uniaxial strain condition (constant radial strain). In both cases, "pore pressure" remains constant, equal to the atmospheric pressure during the loading phases, and near atmospheric pore pressure (less than 10 bars) when measuring permeability. The loading is performed step by step,

between the permeability measurements stages, as shown in figure 2. Permeability is measured at the end of each of these stages, after a stabilization period. Gas flow is parallel to the sample axis. Tests were run at room temperature.

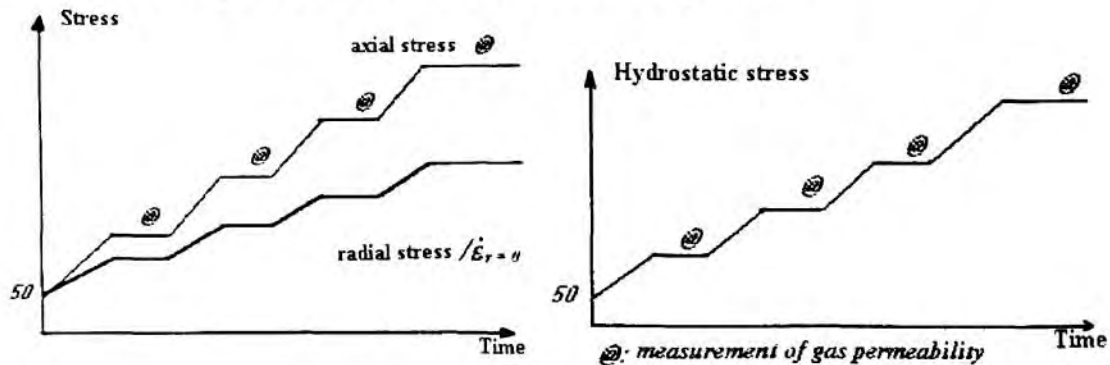


Figure 2 : Loading scheme for gas permeability testing

## Results and Discussion

These tests aimed at determining the gradual evolution of permeability and porosity when effective stresses increase during depletion. These depressurizations are significant : in the sandstones reservoir, reaching up to 1000 bars (resp. 600 bars in the carbonates reservoir). Samples were first subjected to hydrostatic loading followed by uniaxial loading, except sample S1, for which the loading sequence was reversed. Table 2 summarizes the results.

Sample	S1	S2	S3	C1	C2
<b>Solid density</b>	2.68	2.66	2.66	2.85	2.86
<b>Porosity - unconfined - (fract.)</b>	0.126	0.177	0.131	0.076	0.088
<b>Porosity reduction (%)</b>					
$\sigma_{\max}$ - hydrostatic	7.7	5.5	7.2	2	1.6
$\sigma_{a \max}$ - uniaxial	7	2.7	3.6	0.95	1
<b>Gas permeability (<math>K_{gKL}</math>) (mD)</b>					
$\sigma=50$ bars - hydrostatic (1)	$1.6 \cdot 10^{-2}$	$1.7 \cdot 10^{-1}$	$3.1 \cdot 10^{-2}$	$8.4 \cdot 10^{-3}$	$8.6 \cdot 10^{-1}$
$\sigma_{\max}$ - hydrostatic (2)	$6.5 \cdot 10^{-3}$	$7.3 \cdot 10^{-2}$	$1.1 \cdot 10^{-2}$	$7.4 \cdot 10^{-3}$	$7.2 \cdot 10^{-1}$
After unloading - $\sigma_a = 50$ bars	-	$1.3 \cdot 10^{-1}$	-	-	-
$\sigma_a=50$ bars; $\sigma_r=50$ bars (3)	$2.2 \cdot 10^{-2}$	$1.3 \cdot 10^{-1}$	$2.0 \cdot 10^{-2}$	$8.5 \cdot 10^{-3}$	$7.9 \cdot 10^{-1}$
$\sigma_{a \max}$ - uniaxial (4)	$1.2 \cdot 10^{-2}$	$8.9 \cdot 10^{-2}$	$1.2 \cdot 10^{-2}$	$8.1 \cdot 10^{-3}$	$7.3 \cdot 10^{-1}$
<b>Kg reduction (%)</b>					
(1-2)/(1)	61	57	65	12	16
(3-4)/(3)	45	32	40	5	8

$\sigma_{a \max} = 1200$  bars ;  $\sigma_{\max} = 1200$  bars : S-type samples

$\sigma_{a \max} = 700$  bars ;  $\sigma_{\max} = 700$  bars : C-type samples

Table 2 : Permeability and porosity variations : uniaxial vs. hydrostatic tests

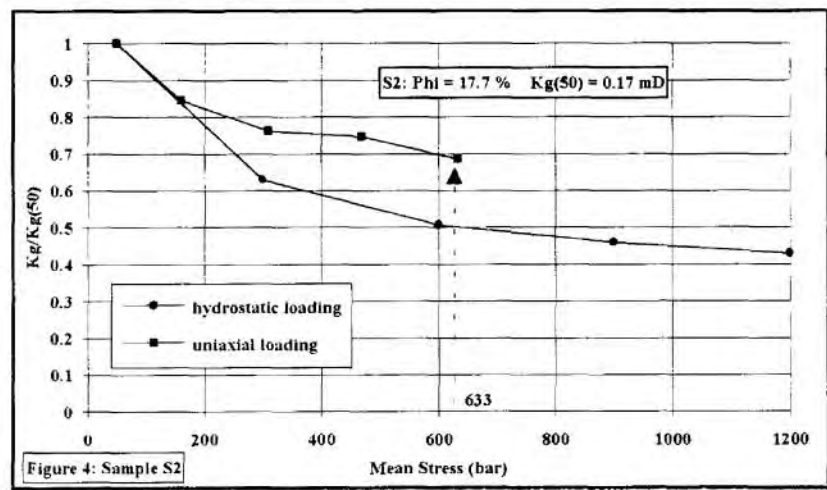
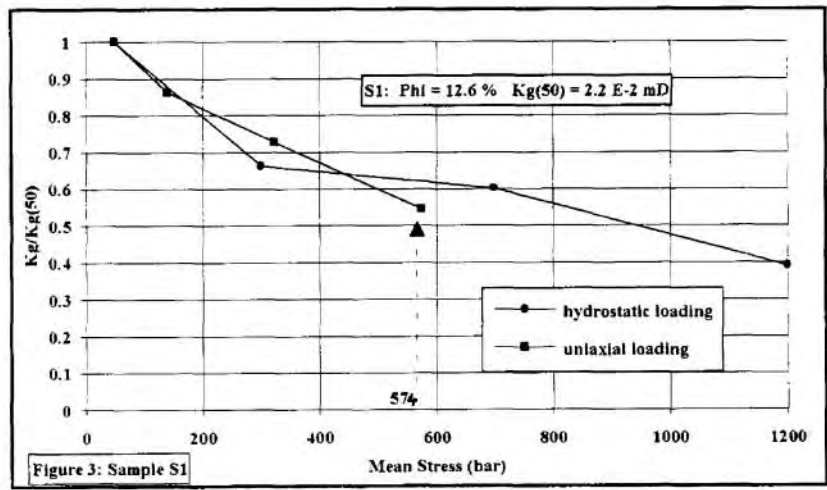


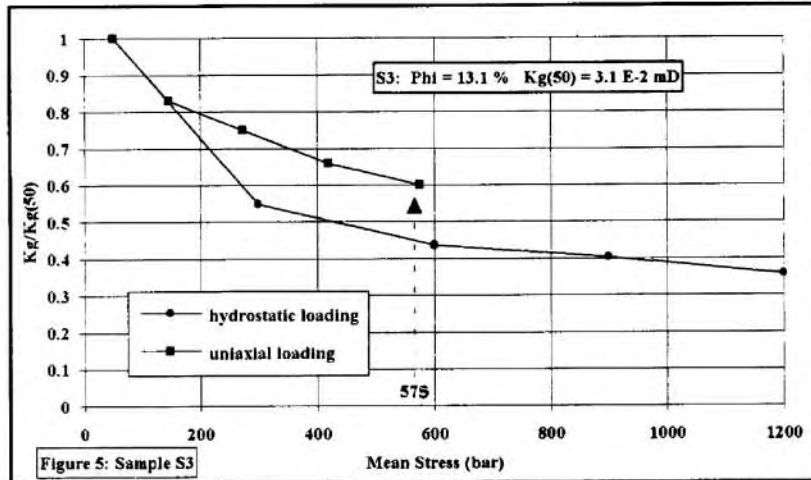
Some noticeable minor differences in the initial permeabilities come from some irreversible deformations of samples after the first loading-unloading cycle. Figures 3 to 7 display the permeability variation with mean stress increase.

"Mean stress" stands for the ratio  $(\sigma_{axial} + 2 \sigma_{radial})/3$ , where the axial and radial stresses are measured during an experiment.

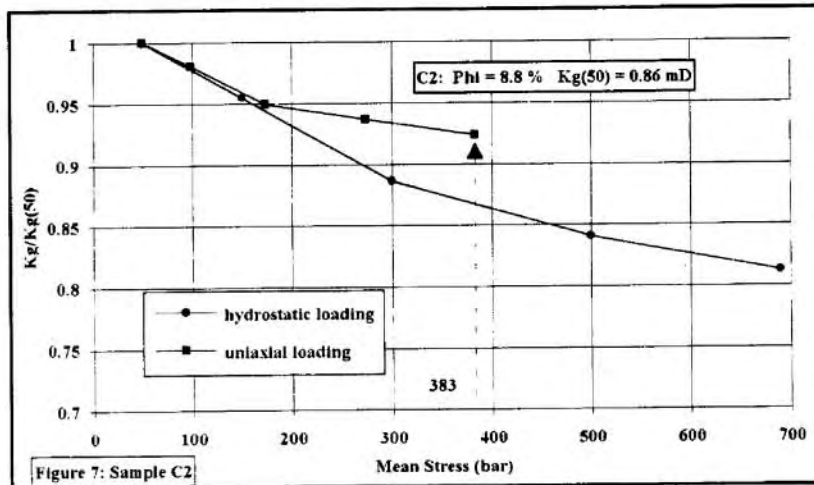
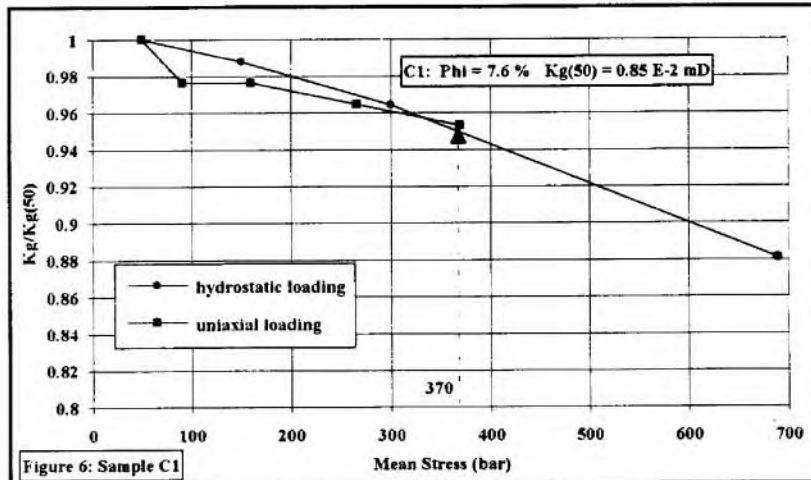
The curves clearly exhibit two regimes for the permeability variation. A sharp decrease in permeability is observed at first, followed by a smooth quasi-linear permeability reduction, except for sample C1 in which the decline in permeability is rather linear during the entire loading phase. The behavior of C1 likely originates from the composition of the rock which generates specific changes in rock deformations mode. Concerning the two groups of rocks, a major difference is to be pointed out between the behavior of the carbonates and sandstones. The former have rather minor permeability reductions (from 5% to 8%, during the uniaxial tests), whereas the latter permeability decreases range from 32% to 45%.

**Normalized Permeability vs Mean Stress for sandstone samples :**





**Normalized Permeability vs Mean Stress for carbonate samples :**



The permeability decrease is more pronounced during hydrostatic loadings, from 57% to 65%, compared with 32% to 45% during uniaxial compaction (figures 3 to 7).

Differences between hydrostatic and uniaxial tests are also noticeable, though slightly reduced, at the upper level of stresses during uniaxial compaction, except for samples S1 and C1 in which permeability declines are nearly equal during both tests (table 3). Therefore, even though the actual effective stresses (in the sense of Biot's theory) were known at the initial state and final state in the reservoir deformations, and if the tests were run accordingly, differences in permeability variations between the two loading paths would still remain. This emphasizes the need for representative measurements at in-situ conditions, as previously recommended by Holt (1989), Rhett and Teufel (1992).

Sample Orientation	S1 V	S2 V	S3 V	C1 V	C2 V
Upper Mean Stress Uniaxial Compaction	574	633	575	370	383
Permeability reduction (%)					
Uniaxial	45	32	40	5	8
Hydrostatic	39	50	56	5	14

Table 3 : Permeability reductions at uniaxial compaction upper mean stress

The experiments show that the lower the intrinsic permeability, the higher the reduction (samples S1 and S3). This observation is confirmed by additional tests performed on higher permeabilities S-type samples (6.5 mD and 12.6 mD) which experienced the same loading paths. Permeabilities decrease by less than 21% (uniaxial loading) and 29% (hydrostatic loading), as reported in table 4 below. These are half the reductions in the lower permeability sandstones.

Sample Orientation	S4 V	S5 V
Porosity - unconfined - (fract.)	0.222	0.187
Brine permeability (Kw) (mD)		
$\sigma_a = 40$ bars; $\sigma_r = 40$ bars (1)	-	6.45
$\sigma_a = 150$ bars; $\sigma_r = 50$ bars (1)	12.60	-
$\sigma_a = 1000$ bars <b>uniaxial</b> (2)	10.0	5.40
After unloading - $\sigma_a = 150$ bars	10.85	-
$\sigma = 50$ bars <b>hydrostatic</b> (3)	11.30	-
$\sigma = 1000$ bars <b>hydrostatic</b> (4)	8.0	4.70
Kw reduction (%)		
(1-2)/(1)	21	16
(3-4)/(3)	29	-
(1-4)/(1)	-	27 *

\* likely slightly overestimated

Table 4 : Liquid permeabilities on S-type specimens



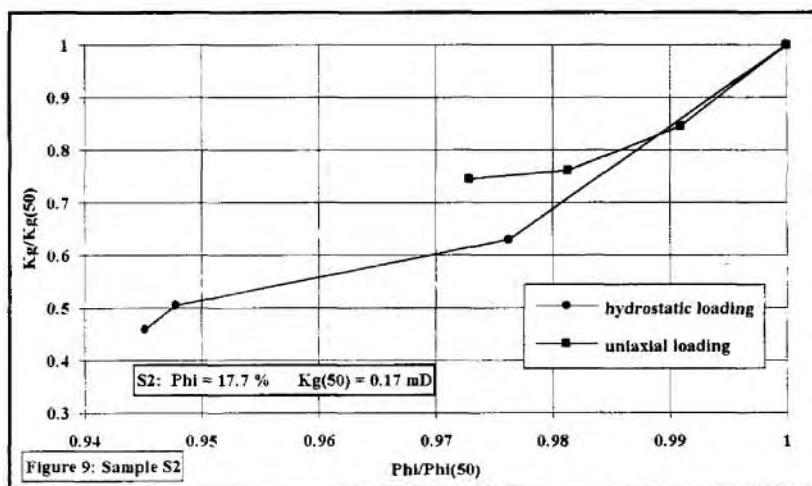
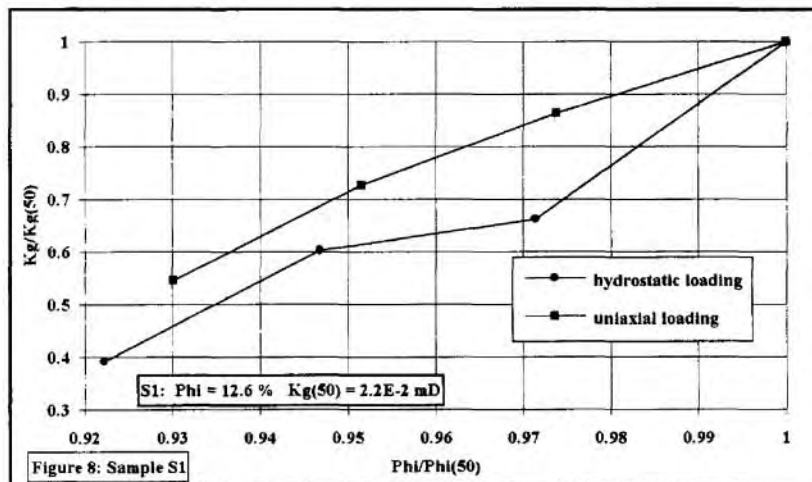
However, carbonate specimens give rather different results : the higher permeability sample C2 (two orders of magnitude higher than C1) shows higher reductions than sample C1. Scanner actually reveals that C2 contains a crack, which could explain this discrepancy. Such cracks are very common in this facies.

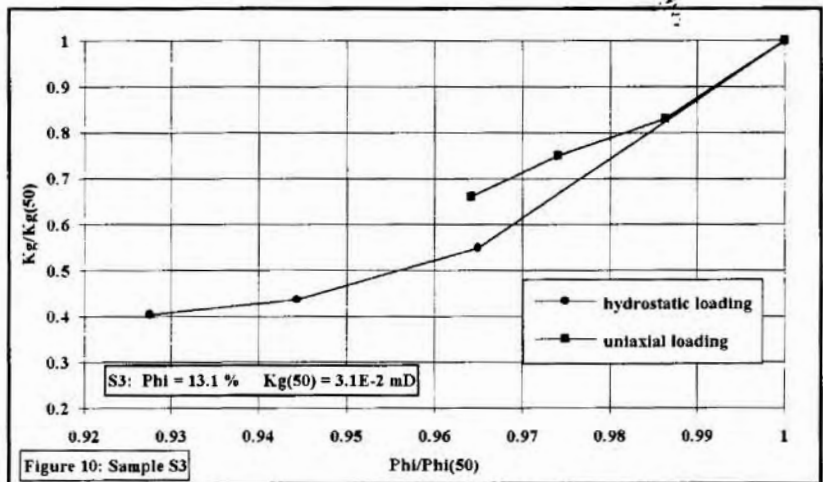
These measurements also underline that, for a given rock type, the lower the unconfined porosity, the lower the intrinsic permeability.

As far as porosity reduction is concerned, the plots  $K_g/K_g(50)$  in function of  $\Phi/\Phi(50)$  (figures 8 to 12) confirm the observations and trends above. But, once again, samples S1 and C1 behave differently. The porosity reduction during the hydrostatic loading is about twice that recorded during uniaxial loadings (S2, S3, C1 and C2). However, sample S1 shows nearly equal variations in both cases even though the uniaxial reduction is slightly lower.

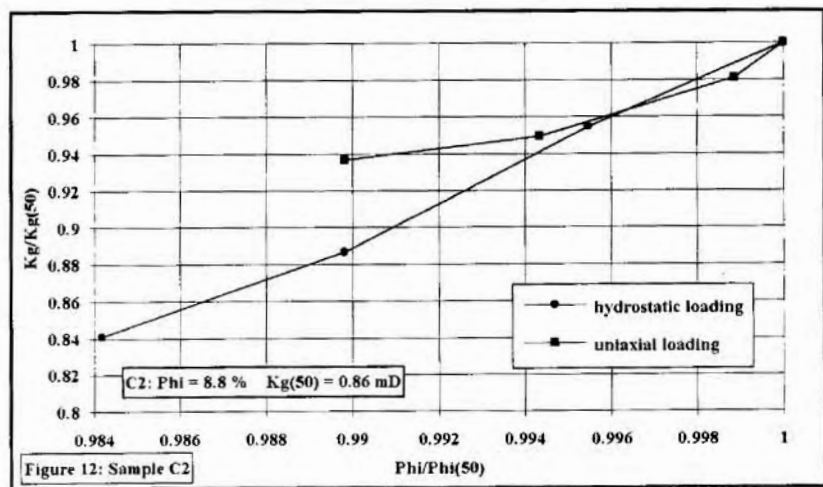
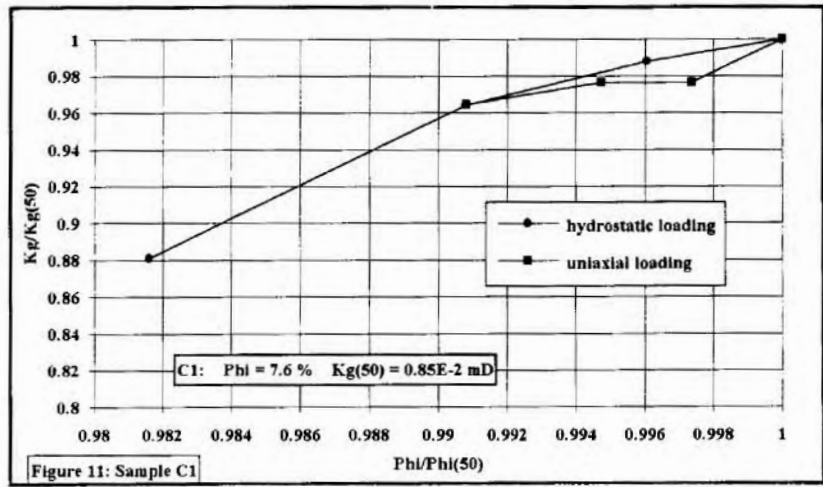
Permeability reductions are consistent with deformations : on C-type samples, deformations are very small leading to far lower permeability reductions than for S-type samples.

**Normalized Permeability vs Porosity Reduction for sandstone samples :**





**Normalized Permeability vs Porosity Reduction for carbonate samples :**



## Conclusions

This study on tight high pressure reservoir rocks clearly demonstrates that uniaxial compaction tests generate lower reductions of both matrix permeability and porosity than hydrostatic experiments. Performing hydrostatic tests alone will have resulted in over-estimating variations of these rock properties, therefore being very misleading in reservoir engineering studies. Hydrostatic compaction is less representative of the actual reservoir states of stresses and reservoir deformations. A better understanding of the effects of in-situ stresses and deformations on permeability can have a significant influence on the permeability cutoff level derived and the Net/Gross pay estimate.

Consequently, in an attempt to give reliable, accurate permeability and porosity in-situ and during reservoir depletion, tests representative of in-situ conditions (likely uniaxial compaction or triaxial measurements) should be preferred to routine analyses, which results should not be used without corrections from in-situ reservoir conditions. However, the comparison between low permeability sandstones and carbonates indicates that their behaviors, with regards to both permeability and porosity reductions function of increasing stresses, are different. Non-homogeneous and isotropic cores could also be very confusing. As a consequence, no general relationship or correction factors can be derived to predict permeability reduction on a typical facies without the help of reliable and representative experiments.

## Acknowledgments

This work was performed at Elf Aquitaine Production with the contribution of A.E.I.A. company. The authors acknowledge permission from Elf Aquitaine Production to publish this paper. They wish to acknowledge a number of people for their help to the work presented here. In particular, B. Marlin for "stimulating" technical discussions, B. Labeyrie and J. Gadioux who performed the core analyses.

## Nomenclature

<b>A</b>	core cross sectional area
<b>b</b>	gas slippage factor
<b><math>\beta</math></b>	inertial resistance coefficient
<b>cgp</b>	gas compressibility
<b><math>\epsilon_r</math></b>	radial strain
<b><math>\epsilon'</math></b>	$d\epsilon/dt$
<b><math>\phi</math> or <b>phi</b></b>	porosity
<b>Kg</b>	gas permeability
<b>KgKl</b>	Klinkenberg corrected gas permeability

<b>K<sub>w</sub></b>	liquid permeability
<b>L</b>	core length
<b>μ</b>	gas viscosity
<b>P</b>	pressure
<b>Q</b>	gas mass flow rate
<b>ρ</b>	gas density
<b>σ</b>	effective stress (or net confining pressure)
<b>σ<sub>i</sub></b>	initial experimental confining pressure
<b>σ<sub>a</sub>, σ<sub>r</sub></b>	axial stress, radial stress
<b>σ'</b>	loading rate (dσ/dt)
<b>v</b>	gas velocity
<b>V</b>	vessel volume
<b>V<sub>p</sub></b>	pore volume

#### Subscripts

<b>1 ; 2</b>	inlet; outlet
<b>m</b>	mean
<b>g</b>	gas

#### Conversion Factors

bar x 10 = 1 MPa

mD x 9,869233.10<sup>-4</sup> = 1 μm<sup>2</sup>

#### References

BOURBIE T., WALLS J.D., Pulse Decay permeability analytical solution and experimental test, Society of Petroleum Engineers, Journ. Oct. 1982, p 719-721.

HSIEH P.A., TRACY J.V., NEUZIL C.E., BREDEHHOEFT J.E., and SILLIMAN S.E., A transient laboratory method for determining the hydraulic properties of tight rocks, Int. J. Rock Mech. Min. Sci. & Geomech., 1981, Vol. 18, p 245-252.

HOLT R.M., Permeability reduction induced by a nonhydrostatic stress field, Society Petroleum Engineers, 1989, San Antonio.

IFFLY R., Etude de l'écoulement des gaz dans les milieux poreux, Revue de l'Institut Français du Pétrole, juin 1956, Vol. 11 n°6.

JONES S.C., A rapid accurate unsteady-state Klinkenberg permeameter, Society of Petroleum Engineers, Journ. Oct. 1972, p 383-397.

JONES S.C., Recommended Practice for determining permeability of porous media, American Petroleum Institute, 1991, Draft version.

McPHEE C.A., ARTHUR, K.G., Klinkenberg permeability measurements : problems and practical solutions, Society of Core Analysts, 1991, London.

RHETT D.W., TEUFEL L.W., Effect of reservoir stress path on compressibility and permeability of sandstones, Society of Petroleum Engineers, 1992, Washington DC.



